MODELING GROWTH PATTERN FORMATION IN A VERTICALLY ORIENTED THIN-LAYER CELL ELECTRODEPOSITION

E. Mocskos[*]**, G. Gonzalez**[*]**, G. Marshall**[*§]**, S. Dengra**[*]**, and F. V. Molina**[†§]
[*]Laboratorio de Sistemas Complejos
Departamento de Computación, Facultad de Ciencias Exactas y Naturales (FCEyN)
Universidad de Buenos Aires, Ciudad Universitaria,
Pabellón I, (C1428EGA) Buenos Aires, Argentina.
web page: http://www.lsc.dc.uba.ar
[†]Departamento de Química Inorgánica, Analítica y Química Física,
Facultad de Ciencias Exactas y Naturales (FCEyN),
Universidad de Buenos Aires, Ciudad Universitaria,
Pabellón I, 1428 Buenos Aires, Argentina.
[§] Consejo Nacional de Investigaciones Científicas y Técnicas, 1428 Buenos Aires, Argentina

Key Words: HPC, Cluster, Perfomance, Parallel Computing, Beowulf, Finite Differences

Abstract. *Electrodeposition in a thin cell (ECD) in a vertical position, with the cathode above the anode, yields a growth pattern formation whose signature is a dense branched morphology. However, detailed analysis of front evolution reveals a complex competition between neighboring branches leading to a locally fluctuating growth. Here we study the nature of this quasi equilibrium growth through a new macroscopic model and its numerical simulation. The model, based on first principles, uses the Nernst-Planck equations for ion transport, the Poisson equation for the electrostatic potential, the Navier-Stokes equations for the fluid flow and a new growth model, based on a Dielectrical Aggregation Model (DBM), for deposit growth. Numerical simulations in realistic 3D cells using serial and parallel computing are presented; in the latter use is made of domain decomposition techniques with a strongly implicit iterative method implemented in a Beowulf cluster under MPI and Linux. This allows the utilization of very fine grids with a more realistic physical parametrization and results in a robust scalable algorithm attaining almost linear speedup. Theory and simulations suggest the detachment of the leading branch from its neighbors, an enlargement of its tip in the form of a mushroom, and the presence of vortex rings and vortex tubes wrapping the dendrite tip, in qualitative agreement with experimental observations.*

1 INTRODUCTION

In a thin-layer cell electrochemical deposition (ECD) experiment, the electrolytic cell consists of two glass plates sandwiching two parallel electrodes and a metal salt electrolyte. A voltage difference applied between electrodes produces a ramified deposit by reduction of the metal ions. Depending in the cell geometry, its orientation relative to gravity, electrolyte concentration, cell voltage and other parameters, the deposit can be fractal, densely branched or dendritic. ECD has become a paradigmatic model for the study of growth pattern formation (GPF), that is, the unstable growth of interfaces.[1–25]

In thin-layer cell electrochemical deposition (ECD) experiments, dendrite growth is accompanied by a complex physicochemical hydrodynamic ion transport process. Ion transport is mainly governed by diffusion, migration and convection, and convection is mostly driven by coulombic forces due to local electric charges and by buoyancy forces due to concentration gradients that lead to density gradients.

Convection certainly increases ECD complexity and it is natural to try to reduce its influence. Several ways have been proposed with this objective in mind.[12,13,22,26–28] In particular, in,[12] ECD experiments in which the cell is oriented vertically relative to gravity were examined. The authors found that, when the cathode (and low density fluid) is above the anode (and high density fluid), the invasion of the cell by the gravity induced rolls can be avoided while electroconvection remains. When dendrites are present, horizontal concentration gradients drive convection near the growing tips, a competition emerges in which convective motion feeds branches lagging behind until they reach the leading branches. According to the authors, this mechanism inhibits competition leading to a uniform front rather than a hierarchy of branch sizes as seen in horizontal cells.

In the vast majority of previous ECD theoretical models with cells in the horizontal position, a binary electrolyte, fixed electrodes and potentiostatic conditions were assumed. Experimental evidence indicates that more realistic modeling should take into account proton migratory fronts[12,20,29–34], a reasonable growth law and boundary conditions for galvanostatic regimes. An effort in these directions were the works in,[4,32,33] where 1D ECD models, with cells in the horizontal position, with a linear growth law or with three ion electrolytes under constant voltage and steady state regimes were presented. The linear growth law was based upon the experimental evidence of several researchers showing that in many cases the deposit growth speed is equal or similar to the anion drift speed in the relatively unperturbed solution ahead of the growing tip (see for instance,[4]) and in the assumption of dense branched morphology.[35]

It is clear from the previous discussions the need for a fully three-dimensional model of ion transport taking into account a three-ion electrolyte, convective effects and a realistic aggregation model, for describing ECD problems with cells in the horizontal position. But this is, indeed, a formidable task.

A first step towards that goal was presented in,[25] and consisted in a simplified 1D macroscopic model for an ECD experiment in an horizontal cell taking into account a three-ion electrolyte and a linear growth law as the aggregation model. The model revealed new insights of

the fronts interaction and time scaling. However, the need for neglecting convective effects in ECD with cells in horizontal position was a limitation of the model.

In a more recent paper,[36] experimental measurements of ECD in cells in the vertical position with the cathode above and below the anode and a 3D theoretical model was presented. The model revealed useful insights of ECD in vertical cells but was limited to binary electrolytes in the absence of dendrite growth. The results of that work show that global convection was suppressed and therefore a one dimensional analysis neglecting convection could be attempted. Accordingly, this study was presented in.[37] Again, this model gave new insights of the ECD problem but clearly it cannot handle local growth fluctuations as described in.[12, 36]

The aim of this paper is to go one step further in describing conditions in a vertical cell with the cathode above anode, extending the works in[12] and in,[36] in particular addressing the local growth fluctuations by means of the introduction of a theoretical 3D model with a new aggregation model and comparison with experimental measurements. Simulations are carried up in serial and parallel architectures.

The plan of the paper is the following. The phenomenological model and experimental results are presented in Section 2. Section 3 presents the theoretical model and numerical simulations in a serial and parallel machines. The final section draws some general conclusions.

2 THE PHENOMENOLOGICAL MODEL AND EXPERIMENTAL RESULTS

In what follows we present the phenomenological model for a cell in a vertical position (the experimental setup is the same as that presented in[25]). In an ECD experiment in a vertical cell (with the cathode above the anode), when the circuit is closed, current starts flowing through the cell and ion concentration boundary layers develop near each electrode. At the anode the concentration is increased above its initial level due to the transport of anions towards, and the dissolution of metal ions from the anode. At the cathode, the ion concentration is decreased as metal ions are reduced and deposited out and anions drift away. These concentration variations lead to density variations, and therefore to concentration fronts at the electrodes. In this configuration the high density fluid is below the low density fluid, hence a stable stratified flow emerges in which gravitoconvection is suppressed. Stratification remains stable as long as there is no growth of dendrites. This configures a globally stable flow in which there is no convection: the cathodic and anodic concentration fronts being lighter and heavier, respectively, than the fluid adjacent, do not detach from their respective electrodes, and the absence of dendrites precludes electroconvection. During this initial period, ion transport is mainly diffusive and migratory and cation depletion at the cathode is supposed uniform. Simultaneously, in a very narrow region near the cathode a local charge develops, giving rise to local electric forces initially pointing towards the cathode.

After a few seconds, an instability develops, triggering the growth of a deposit at the cathode. The deposit develops as a three-dimensional (3D) array of thin porous metallic filaments. Electric forces concentrate at the tips; each porous filament allows fluid to penetrate its tip and to be ejected from the sides, forming a vortex ring driven by the electric force. But as soon as dendrite appears stratification breaks down because the fluid concentration surrounding a down-

ward growing dendrite tip diminishes, creating an horizontal concentration gradient and thus, locally gravitoconvection. Clearly, the presence of dendrites generates a vortex tube driven by gravity which sums to the vortex ring driven by local electric charges. In the resulting growth competition, gravitoconvection supplies branches lagging behind until they attain the leading branches. The global result is a rather uniform deposit front with local dendrite growth fluctuations. An example of this behavior is presented in Figure 1 that shows schlieren snapshots of the evolution of the deposit front (dark pixels) and the cathodic and anodic concentration fronts (light pixels). The deposit front looks rather smooth in the average, dendrite tips surrounded by tenuous concentration arches joining neighboring tips. The shape of the arches is the result of electroconvection and gravitoconvection.
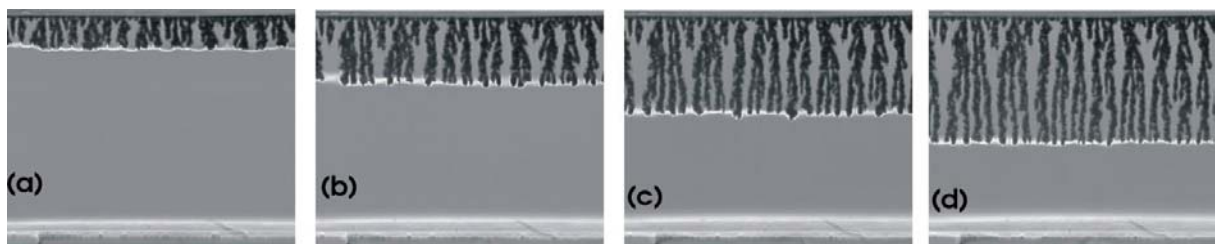
Figure 1: Schlieren images of ECD in a vertical oriented cell at (a) 80s, (b) 160s, (c) 240s and (d) 320s. Copper sulfate solution concentration is 0.1M, the cell dimensions are $70 \times 10 \times 0.2 \, \text{mm}^3$ and the applied constant current is 7.5mA.

However, an enlarged image of a small section of the dendrite front shows the fluctuating growth evolution of a branch and its neighbors as presented in Figure 2: once a branch is detached from its neighbors, its tip enlarges adopting the shape of an inverted mushroom; the situation continues until the lagging branches catch up with the leading branch. The following explanation is advanced. As the leading branch detach from its neighbors, its local charge increases, the ion transport becomes more electroconvective dominant, which in turn tends to accelerate the leading branch. However, simultaneously, a buoyancy force develops, a force that is proportional to the size of the leading branch detachment. An increase in the buoyancy force feeds flow to the neighboring branches accelerating them (buoyancy brings higher concentration solution to the lagging branches accelerating them). There is another angle to this description which merits a detour: during its detachment, the leading branch encounters a region of higher concentration surrounding its front and sides that increases the aggregation giving rise to a mushroom like shape. In turn, this mushroom effect decreases the local electric force at the tip due to the local charge spread. How this affects the global balance is still a matter of conjecture.

To study in detail the behavior at the tip of a branch we present an ECD experiment in a vertical cell (cathode above anode) in which a small detachment (fluctuation) of a branch from its neighbors is represented by a small protruding spike in an otherwise flat cathode. The result is shown in figure 3 where convection is visualized with 200 snapshots of micron sized tracer particles, spanning an interval of 20 s, superposed to show their motion. The resulting motion is the effect of the superposition of two pairs of counter-rotating vortices due to local buoyancy
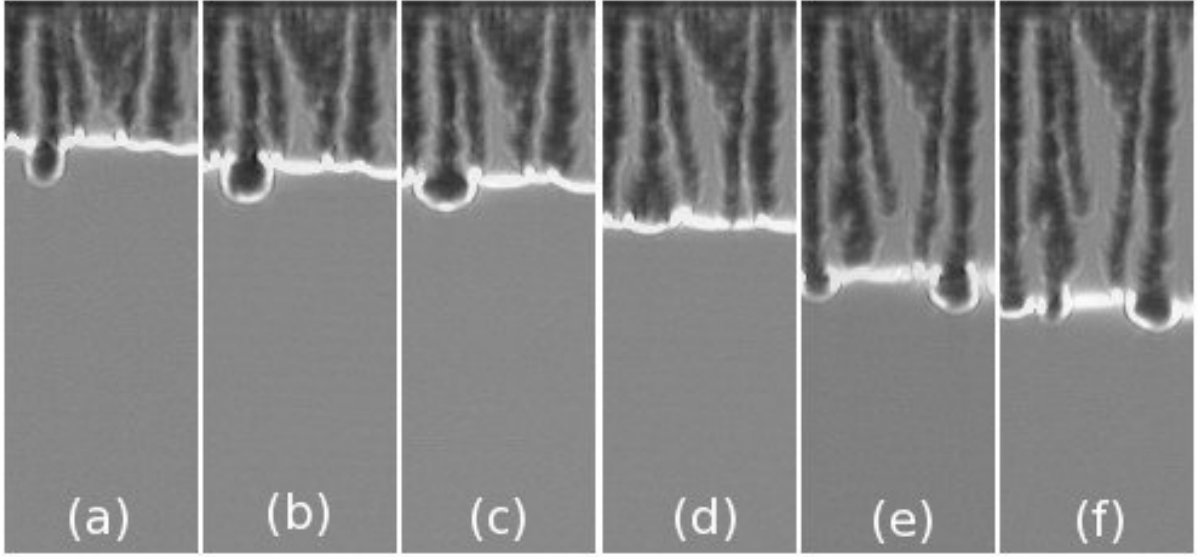
Figure 2: Enlarged Schlieren images of ECD in a vertical oriented cell at (a) 160s, (b) 185s, (c) 200s, (d) 250s, (e) 300s and (f) 325s showing the growth fluctuation. Copper sulfate solution concentration is 0.1M, the cell dimensions are $70 \times 10 \times 0.2\,\mathrm{mm}^3$ and the applied constant current is 7.5mA.

and local electric forces.

3   THEORETICAL ANALYSIS AND NUMERICAL SIMULATIONS

Ion transport in thin-layer ECD can be described with a mathematical model based on first principles,[38–41] including the Nernst-Planck equations for ion transport, the Poisson equation for the electric potential, and the Navier-Stokes equations for the fluid flow. The 3D dimensionless system of equations can be written as

$$\frac{\partial C_i}{\partial t} = -\nabla \cdot \mathbf{j}_i \tag{1}$$

$$\mathbf{j}_i = -M_i C_i \nabla \phi - \frac{1}{Pe_i} \nabla C_i + C_i \mathbf{v} \tag{2}$$

$$\nabla^2 \phi = Po \sum_i z_i C_i \tag{3}$$

$$\frac{\partial \boldsymbol{\zeta}}{\partial t} + \nabla \times (\boldsymbol{\zeta} \times \mathbf{v}) = \frac{1}{Re} \nabla^2 \boldsymbol{\zeta} + \sum_i \left[G_e z_i (\nabla \phi \times \nabla C_i) \right. \\ \left. - G_{g_i} \nabla \times \left(C_i \frac{\mathbf{g}}{g} \right) \right] \tag{4}$$
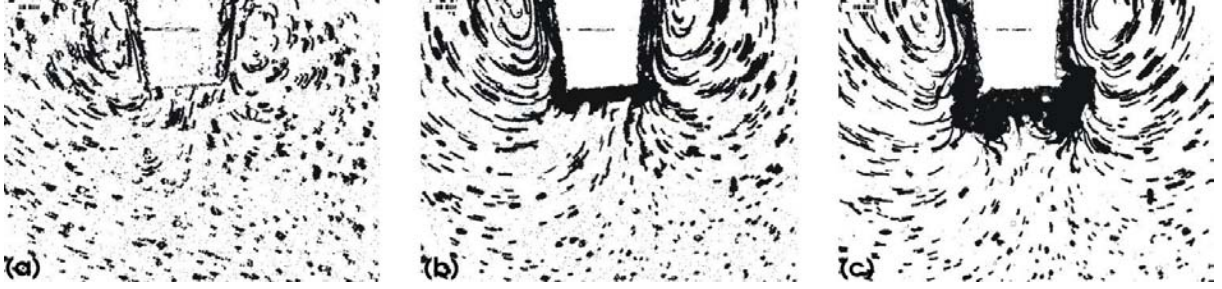
Figure 3: Visualization of 1μm sized particle trajectories near the cathode spike (amplified). To show the motion of tracer particles, 200 digital images were superimposed in the intervals (a) 0-20s, (b) 20-40 and (c) 40-60s. Copper sulfate solution concentration is 0.1M with 30% glycerol in weight, the cell dimensions are $70 \times 10 \times 0.127 \, \text{mm}^3$, the applied constant current is 2mA and the spike dimensions are $1 \times 0.5 \times 0.127 \, \text{mm}^3$

$$\boldsymbol{\zeta} = -\bigtriangledown^2 \boldsymbol{\Psi} \tag{5}$$

$$\mathbf{v} = \bigtriangledown \times \boldsymbol{\Psi} \tag{6}$$

Here C_i and $\mathbf{j}_i$ are the dimensionless concentration and flux of an ionic species i (for a ternary electrolyte such as ZnSO$_4$ /H$_2$SO$_4$, $i=$ C, A and H, standing for zinc, sulphate and hydrogen ions); $\mathbf{v}$, ϕ, $\boldsymbol{\zeta}$ and $\boldsymbol{\Psi}$ are the dimensionless fluid velocity, electrostatic potential, vorticity vector and velocity potential vector, respectively; $\mathbf{g}/g$ is a unit vector pointing in the direction of gravity. The quantities $M_i = \mu_i \Phi_0/x_0 u_0$, $Pe_i = x_0 u_0/D_i$, $Po = x_0^2 C_0 e/\epsilon\Phi_0$, $Re = x_0 u_0/\nu$, $G_e = eC_0\Phi_0/\rho_0 u_0^2$ and $G_{g_i} = x_0 C_0 g\alpha_i/u_0^2$, stand for the dimensionless numbers Migration, Peclet, Electric Poisson, Reynolds, Electric Grashof and Gravity Grashof numbers, respectively. The quantities z_i, μ_i, and D_i are, respectively, the number of charges per ion, mobility and diffusion constants of an ionic species i; μ_i and z_i are signed quantities, being positive for cations and negative for anions; g is the dimensional gravitational acceleration; e is the electronic charge, ϵ is the permittivity of the medium and ν is the kinematic viscosity. x_0, u_0, ϕ_0, C_0, and ρ_0 are reference values of the length, velocity, electrostatic potential, concentration, and fluid density, respectively. For system closure, a Boussinesq-like approximation has been used for the fluid density: $\rho = \rho_o(1 + \Sigma_i \alpha_i \Delta C_i)$, where $\alpha_i = \frac{1}{\rho_o}\frac{\partial \rho}{\partial C_i}$.

System (1-6), with appropriate initial and boundary conditions, is valid in a space-time domain defined by $\mathbf{G} = [\boldsymbol{\Omega}(\mathbf{t})\mathbf{x}(\mathbf{0}, \mathbf{t})]$, where Ω is a three-dimensional region with boundary $\Gamma(t)$; this boundary moves with speed proportional to the norm of the flux $\mathbf{j}_i$. The boundary conditions for the velocity potential vector are discussed, for instance, in:[42] in a plane impermeable surface, the vector is normal to the surface and its gradient is zero; at nonslip surfaces, the tangential derivative of the velocity components are zero.

The computational model solves the previous 3D system of equations, for each time step, in a fixed or variable domain, in a 3D uniform lattice, using finite difference and deterministic relaxation techniques. Its solution is obtained via the system of difference equations:

$$\mathbf{W}_k^{n+1} = \sum_j \mathbf{a}_j \mathbf{W}_j^n \tag{7}$$

where j represents the nearest-neighbor site of the site k; the summation ranges over all nearest-neighbor sites; $\mathbf{W}_k$ is a vector-valued function whose components are the concentrations C_i, the electrostatic potential ϕ, the vorticity vector $\boldsymbol{\zeta}$ and velocity potential vector $\boldsymbol{\Psi}$; and $\mathbf{a}_j$ is a diagonal matrix whose elements contain the nonlinear coefficients of the discretized equations. The resulting solution $\mathbf{W}_k^{n+1}$ is then used to advance the interface with a dielectrical breakdown model (DBM).[43] The interface is moved at random, proportionate to the flux of cations, i.e.,

$$p_k = \frac{|\mathbf{j}_{c_k}|}{\sum_i |\mathbf{j}_{c_i}|} \tag{8}$$

where k is a nearest neighbor site to the interface, p_k is the probability of selecting the nearest neighbor site k to advance the interface, the summation is over all nearest neighbor sites i to the interface, and $\mathbf{j}_{ck}$ is the flux of cations flowing from the neighbor site k into the aggregation.

In the following we present numerical simulations of ECD experiments with the cell in a vertical position with the cathode above the anode and with a spike in an otherwise flat electrode. In all the simulations we assumed a binary electrolyte. Here we describe serial computing results with a moving boundary. Details of the parallel simulations using domain decomposition techniques in a fixed domain implemented on a Beowulf cluster under MPI and Linux are presented in a separate work in this conference (P. Milano, E. Mocskos and G. Marshall, Mejoras en la perfomance de un programa paralelo de fisicoquimica hidrodinamica computacional en un cluster Beowulf heterogeneo, MECOM2005). In that work it is shown that a judicious mix of parallel techniques allow the utilization of very fine grids with a more realistic physical parametrization, resulting in a robust scalable algorithm in which almost linear speedup is attained.

A typical cell is represented by a cubic grid of $240 \times 60 \times 160$ nodes. The dimensionless numbers used are: $M_a = 0.625$, $M_c = 0.42$, $Pe_a = 2.4$, $Pe_c = 3.6$, $Po = 1.9 \times 10^2$, $Re = 2.5 \times 10^{-3}$, $Ge = 1 \times 10^4$, $Gg_a = 2.0 \times 10^4$ and $Gg_c = 1.33 \times 10^4$. These numbers correspond to the experiment presented in figure 3 except for the real Poisson and Electric Grashof numbers (in the order of 1×10^8 and 1×10^{12} cm^{-3}, respectively, see[21]), which cannot be handled, because they produce unstable numerical solutions. All the graphics for the numerical simulations is done with the plotting package *OpenDx*.[44]

Towards a description of the experiment shown in figure 3 we present a simulation in which a solitary dendrite is mimicked by a square spike or finger protruding from the cathode. The results of the evolution of the velocity field superimposed with an anion isoconcentration surface, in a longitudinal cross-section at the cell center, are shown in figures 4 and 5. In these figures, the isoconcentration surface is taken close to the finger growth, thus indicating the growth shape. The figures also show the hydrodynamic pattern near the growth resulting from a composition of the vortex tube driving by local gravitoconvection and the vortex ring driven

by electroconvection. Away from the cathode, there is a stratified flow with a complete absence of convection as in the experiments.
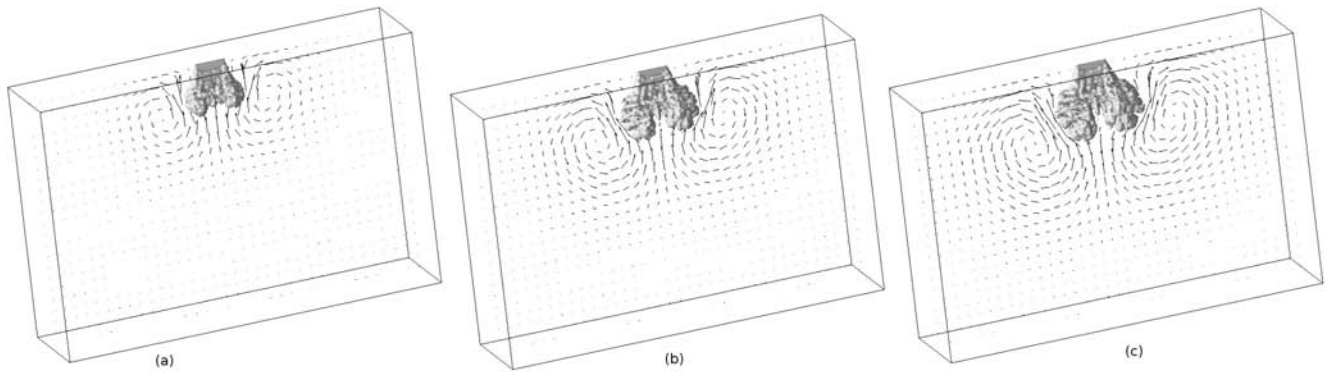
Figure 4: ECD in a vertical cell: simulation near the spike (enlarged): velocity field superimposed with an anion isoconcentration surface at three successive times.
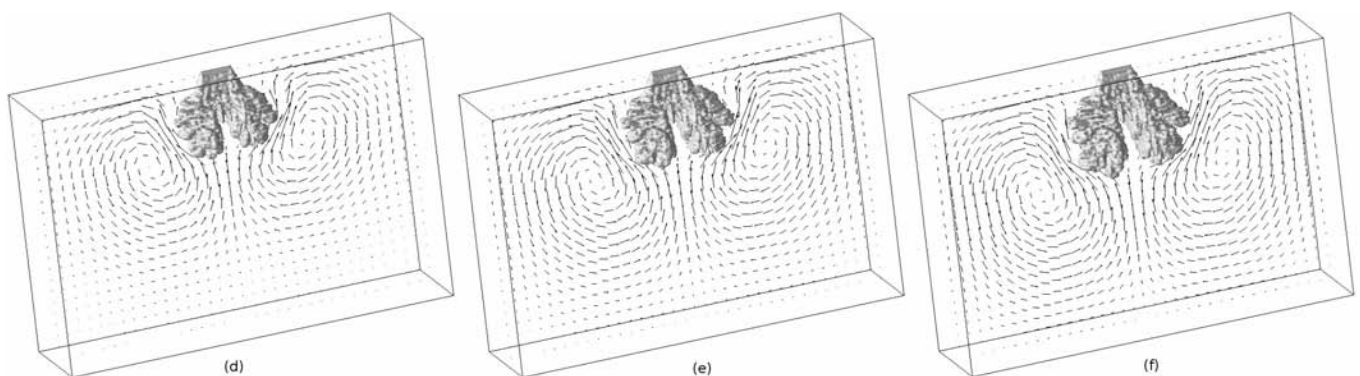
Figure 5: ECD in a vertical cell: simulation near the spike (enlarged): velocity field superimposed with an anion isoconcentration surface at the next three successive times.

4   CONCLUSIONS

We reported experimental measurements of ECD with a cell in the vertical position and the cathode above the anode, and we introduced a 3D theoretical macroscopic model with a stochastic aggregation model for dendrite growth and numerical simulations in serial and parallel machines describing many features of those flows. Parallel simulations using domain decomposition in a Beowulf cluster under MPI and Linux allowed much more realistic physical descriptions. In some of them, almost linear speedup was attained. Our model predicts that when the cathode is above the anode and no growth of dendrites is present, the flow is globally stable. When dendrites are present the fluid concentration near a downward growing tip is lowered

thus generating a vortex tube (driven by gravitoconvection) superposed to a vortex ring (driven by electroconvection) wrapping the dendrite tip (much as in the case of the horizontal cell in which the dendrite tip is surrounded by gravito- and electroconvective vortices, respectively). The region close to the anode is not affected by the growth and remains without convection. This yields a quasi-stable flow regime.

In the presence of dendrites, our model predicts the existence of a vortex ring at the tips of the dendrites, driven by electroconvection, allowing fluid to penetrate at the tip and be ejected from its sides. Local flow at the tips is the result of vortex tube and vortex ring superposition: both have the same sign, that is, at the tip's left and right sides, both vortices are clockwise and counter clockwise, respectively. The simulated growth at the tips of the dendrite exhibits the formation of a mushroom. Such behavior is observed in experiments.

ACKNOWLEDGMENTS

REFERENCES

[1] T. Vicsek. *Fractal Growth Phenomena*. World Scientific, Singapore, 2nd edition, (1992).

[2] F. Argoul, J. Huth, P. Merzeau, A. Arneodo and H. L. Swinney. Experimental evidence for homoclinic chaos in an electrochemical growth process. *Physica D*, **62**(170) (1993).

[3] R. M. Brady and R. C. Ball. Fractal growth of copper electrodeposits. *Nature*, **309**, 225 (1984).

[4] V. Fleury, J. N. Chazalviel, M. Rosso, and B. Sapoval. Experimental Aspects of Electrochemical Deposition of Copper Aggregates. *Phys. Rev. A*, **44**, 6693 (1991).

[5] V. Fleury, J. N. Chazalviel and M. Rosso. Theory and Experimental Evidence of Electroconvection around Electrochemical Deposits. *Phys. Rev. Lett.*, **68**, 2492 (1992).

[6] V. Fleury, J. N. Chazalviel and M. Rosso. Coupling of Diffusion, Migration and Convection in the Vicinity of Electrochemical Deposits. *Phys. Rev. E*, **48**, 1279 (1993).

[7] V. Fleury, J. Kaufman and B. Hibbert. A Mechanism of Morphology Transition in Ramified Electrodeposition. *Nature*, **367**, 435 (1994).

[8] K. A. Linehan and J. R. de Bruyn. A Mechanism of Morphology Transition in Ramified Electrodeposition. *Can. J. Phys.*, **73**, 177 (1995).

[9] V. Fleury, M. Rosso, and J. N. Chazalviel. Electrochemical Deposition Without Supporting Electrolyte. In B. Sapoval F. Family, P. Meakin and R. Wool, editors, *MRS Symposia Proc*, Boston, (1994). Material Research Society.

[10] V. Fleury, M. Rosso and J. N. Chazalviel. Diffusion Migration and Convection in Electrochemical Deposition, Vortex Pairs, Vortex Rings Arches and Domes. In H.D. Merchant, editor, *symposium on "Structure and Properties of Deposits"*, pages 195–217, Warrendale

penn, (1995). 3M (Metals Minerals and Materials Society), TMS Publications.

[11] V. Fleury and J.N. Chazalviel. 2-D and 3-D Convection During Electrochemical Deposition, Experiments and Models. In B. Sapoval F. Family, P. Meakin and R. Wool, editors, *MRS Symposia Proc*, Boston, (1994). Material Research Society.

[12] J. Huth, H. Swinney, W. McCormick, A. Kuhn and F. Argoul. Role of convection in thin-layer electrodeposition. *Phys. Rev. E*, **51**, 3444 (1995).

[13] J. R. de Bruyn. Fingering instability of gravity currents in thin-layer electrochemical deposition. *Phys. Rev. Lett.*, **74**, 4843–4846 (1995).

[14] D. Barkey, D. Watt, Z. Liu, and S. Raber. The role of induced convection in branched electrodeposit morphology selection. *J. Electrochem. Soc.*, **141**(5), 1206 (1994).

[15] C. Leger, J. Elezgaray, and F. Argoul. Experimental demonstration of diffusion-limited dynamics in electrodeposition. *Phys. Rev. Lett.*, **78**, 5010 – 5013 (June 1997).

[16] J. N. Chazalviel. Electrochemical aspects of the generation of ramified metallic electrodeposits. *Phys. Rev. A*, **42**, 7355–7367 (December 1990).

[17] G. Marshall, E. Perone, P. Tarela and P. Mocskos. A macroscopic model for growth pattern formation of ramified copper electrodeposits. *Chaos, Solitons and Fractals*, **6**, 315 (1995).

[18] G. Marshall and P. Mocskos. Growth model for ramified electrochemical deposition in the presenceof diffusion, migration, and electroconvection. *Phys. Rev. E*, **55**, 549–563 (January 1997).

[19] G. Marshall, P. Mocskos, H. L. Swinney and J. M. Huth. Buoyancy and electrically driven convection models in thin-layer electrodeposition. *Phys. Rev. E*, **59**, 2157 – 2167 (February 1999).

[20] S. Dengra, G. Marshall and F. Molina. Growth model for ramified electrochemical deposition in the presenceof diffusion, migration, and electroconvection. *J. Phys. Soc. Japan*, **69**, 963–971 (March 2000).

[21] G. Gonzalez, G. Marshall, F. V. Molina, S. Dengra and M. Rosso. Viscosity effects in thin-layer electrodeposition. *J. Electrochem. Soc.*, **148**(7), C479–C487 (July 2001).

[22] G. Gonzalez, G. Marshall, F. V. Molina and S. Dengra. Transition from gravito- to electroconvective regimes in thin-layer electrodeposition. *Phys. Rev. E*, **65**(5), 051607 (May 2002).

[23] G. Marshall, E. Mocskos, F. V. Molina and S. Dengra. Three-dimensional nature of ion transport in thin-layer electrodeposition. *Phys. Rev. E*, **68**(2), 021607 (August 2003).

[24] S. Dengra. *Experimental and theoretical studies of ion transport in thin-layer electrodeposition cells*. PhD thesis, Departamento de Computación, Universidad de Buenos Aires, (August 2004).

[25] G. Marshall, F. V. Molina and A. Soba. Ion transport in thin cell electrodeposition: modelling three-ion electrolytes in dense branched morphology under constant voltage and current conditions. *Electrochimica Acta*, **50**(16–17), 3436–3445 (May 2005).

[26] M. Rosso, J. N. Chazalviel, V. Fleury and E. Chassaing. experimental evidence for gravity induced motion in the vicinity of ramified electrodeposits. *E. Acta*, **39**(4), 507–515 (1994).

[27] M.Q. Lòpez-Salvans, P. P. Trigueros, S. Vallmitjana, J. Claret, and F. Sagués. Fingerlike

Aggregates in Thin-Layer Electrodeposition. *Phys. Rev. Lett.*, **76**(21), 4062 (1996).

[28] Y. Fukunaka, K. Okano, Y. Tomii, and Z. Asaki. Electrodeposition of copper under microgravity conditions. *J. Electrochem.Soc.*, **145**(6), 1876 (June 1998).

[29] N. Hecker, D. G. Grier, and L. M. Sander. Extended abstracts of a mrs symposium held in boston. In R. B. Laibowitz, B. B. Mandelbrot, and D. E. Passoja, editor, *Symposium on Fractal Aspects of Materials*, Pittsburgh, PA, (1985). Materials Research Society, University Park.

[30] P. Garik, D. Barkey, E. Ben-Jacob, E. Bochner, N. Broxholm, B. Miller, B. Orr, and R. Zamir. Laplace- and diffusion-field-controlled growth in electrochemical deposition. *Phys. Rev. Lett.*, **62**(23), 2703–2706 (1989).

[31] J. R. Melrose, D. B. Hibbert, and R. C. Ball. Interfacial Velocity in Electrochemical Deposition and the Hecker Transition. *Phys. Rev. Lett.*, **65**(1–2), 3009–3012 (1990).

[32] V. Fleury, M. Rosso, and J.-N. Chazalviel. Geometrical aspect of electrodeposition: The Hecker effect. *Phys. Rev. A*, **43**(12), 6908–6916 (1991).

[33] P. Trigueros, J. Claret, F. Mas, and F. Sagues. Pattern morphologies in zinc electrodeposition. *J. Electroanal. Chem.*, **312**, 219–235 (1991).

[34] A. Kuhn and F. Argoul. Influence of chemical perturbations on the surface roughness of thin layer electrodeposits. *Fractals*, **1**(3) (December 1993).

[35] V. Fleury, M. Rosso, and J.N. Chazalviel. Electrochemical Deposition Without Supporting Electrolyte. In R. A. Lowden, J. R. Hellmann, M. K. Ferber, S. G. DiPietro, and K. K. Chawla, editor, *Ceramic Matrix Composites-Advanced High-Temperature Structural Materials*, volume 365, Boston, (1995). Material Research Society.

[36] G. Marshall, E. Mocskos, G. González, S. Dengra, F.V. Molina and C. Iemmi. Stable, quasi-stable and unstable physicochemical hydrodynamic flows in thin-layer cell electrodeposition. *E. Acta*, (in press) (2005).

[37] G. González, A. Soba, G. marshall, F. Molina and M. Rosso. Dense branched morphology in electrochemical deposition in a thin cell vertically oriented. In *4th International Symposium on Electrochemical Processing of Tailored Materials*, Kyoto University, Japan, (October 2005).

[38] A. J. Bard and L. R. Faulkner. *Electrochemical Methods, Fundamentals and Applications*. Wiley, New York, (1980).

[39] J. S. Newman. *Electrochemical Systems*. Prentice Hall, New Jersey, (1973).

[40] Ronald F. Probstein. *Physicochemical Hydrodynamics, An Introduction*. Wiley, New York, (1994).

[41] V. G. Levich. *Physicochemical Hydrodynamics*. Prentice Hall, New Jersey, (1962).

[42] G. D. Mallinson and G. de Vahl Davis. Three-dimensional natural convection in a box: A numerical study. *Journal of Fluid Mechanics*, **83**(1) (1977).

[43] L. Pietronero and H. J. Weismann,. *J. Stat. Phys.*, **36**, 909 (1984).

[44] Opendx. An open source imaging package.